IMEKO 24th TC3, 14th TC5, 6th TC16 and 5th TC22 International Conference
11 – 13 October 2022, Cavtat-Dubrovnik, Croatia

DYNAMIC CALIBRATION OF PRESSURE SENSORS WITH THE USE OF DIFFERENT GASES IN THE SHOCK TUBE

Urh Planko[1], Andrej Svete[2], Jože Kutin[3]

Laboratory of Measurements in Process Engineering, Faculty of Mechanical Engineering, University of Ljubljana, Slovenia, [1] urh.planko@gmail.com, [2] andrej.svete@fs.uni-lj.si, [3] joze.kutin@fs.uni-lj.si

Abstract:
This paper studies the possibilities of increasing the amplitude range of the generated pressure steps in the developed diaphragmless shock tube by using appropriate combination of gases in the driver and driven sections of the shock tube. The measurement results of the generated pressure steps using different combinations of lower- and higher-molecular-weight gases as driver and driven gas are presented. By comparison of the resulting pressure steps generated in the diaphragmless shock tube, the most appropriate combination of the driver and driven gas for generating the largest pressure step amplitudes is determined and discussed.

Keywords: time-varying pressure; primary calibration method; diaphragmless shock tube; different gases

1. INTRODUCTION

The increasing need for accurate measurement of rapidly varying pressures in various industrial applications, such as the automotive industry, the polymer injection, the medical field and the aerospace industry, requires the pressure meters with suitable dynamic properties [1]. In order to achieve metrological traceability for dynamic pressure measurements to the International System of Units (SI), two types of dynamic pressure generators show the highest potential as primary standards for dynamic pressure measurements; drop weight systems and shock tubes. While the drop-weight systems have much higher pressure capacities than shock tubes (from few MPa to 400 MPa), the extremely fast-rising pressure-step changes (of the order of 1 ns) generated within the shock tubes lead to their much higher frequency bandwidths, but are limited to the amplitudes of up to few MPa. Therefore, there is still a gap in generation of the pressure amplitudes that are not covered by any of the two dynamic pressure generators. In this paper we study how to increase the amplitudes of the pressure step generated with the shock tube by using appropriate combinations of the driver and driven gases.

2. DIAPHRAGMLESS SHOCK TUBE

A diaphragmless shock tube, which was developed in the Laboratory of Measurements in Process Engineering at the Faculty of Mechanical Engineering in Ljubljana, consists of two straight gas-filled tubes with the same circular cross-section that are initially separated with the fast-opening valve (FOV): a high pressure driver section and a lower pressure driven section, see Figure 1 [2]-[4].

Figure 1: Developed diaphragmless shock tube

An instantaneous opening of the FOV generates a shock wave that propagates through the driven gas. The reflection of the shock front at the end-wall of the driven section, where the pressure meter under calibration (DUT) is mounted, causes a step change in the pressure at this point. The reference pressure step signal generated at the end-wall of the driven section is defined by the pressure step amplitude and the arrival time of the initial shock front at the end-wall of the driven section. The amplitude of the pressure step can be calculated with the following equation [5]:

$$\Delta p = 2 p_1 \frac{\gamma_1}{(\gamma_1^2 - 1)} \left(M^2 - 1\right) \left(\frac{M^2 \left(3\gamma_1 - 1\right) + 3 - \gamma_1}{M^2 + \frac{2}{(\gamma_1 - 1)}} \right), \quad (1)$$

where $M = V/a_1$ is the end-wall shock wave Mach number, V is the end-wall shock wave velocity, $a_1 = \sqrt{\gamma_1 R_1 T_1}$ is the speed of sound, γ_1 is the adiabatic index, R_1 is the specific gas constant, p_1 is the absolute pressure and T_1 is the absolute temperature; index "1" refers to the initial, stationary conditions of the gas in the driven section. The arrival time of the shock front at the

end-wall t_{wall} which defines the initial time of the pressure step at the end-wall, is calculated as:

$$t_{\mathrm{wall}} = t_{\mathrm{last}} + \int_{x_{\mathrm{last}}}^{x_{\mathrm{wall}}} \frac{\mathrm{d}x}{V(x)}. \quad (2)$$

where t_{last} and x_{last} are the passage time of the shock wave over the last side-wall pressure sensor installed downstream of the driven section and its location, respectively, x_{wall} is the location of the end-wall of the driven section and $V(x)$ is shock wave velocity distribution along the driven section determined using a time-of-flight (TOF) method [2]-[4].

In order to enable the use of different combinations of gases in the driver and driven section of the shock tube without mixing them, the shock tube, which was originally designed to be used with the same gas in the driver and driven section, was upgraded by integrating additional supply shut-off valve in the driven section, see Figure 2. Such mechanical implementation of the shock tube enables quality filling of both shock tube sections with the desired gases by the following procedure. First, the undesired gases from each of the shock tube sections are separately evacuated through the shut-off valves integrated at the end-walls of the both sections (see Figure 3 and Figure 4) by blowing through each section of shock tube with the required gas while holding FOV closed. After closing the end-wall shut-off valves, each of the shock tube sections is separately pressurised to the required pressure through the supply shut-off valves with the desired gas using the pressure controllers. Before the actuation of the FOV, the supply shut-off valves are closed to prevent damage to the pressure controllers connected to them.

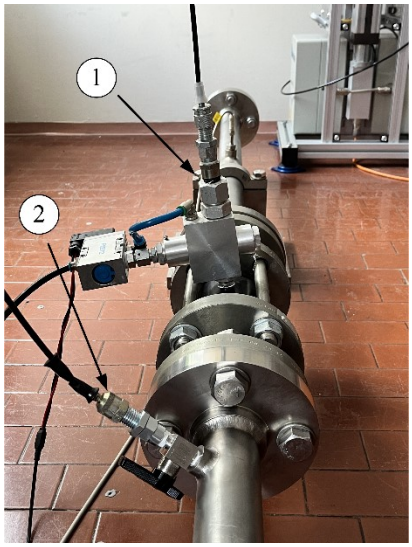

Figure 2: Driver gas supply valve (1) and additionally employed driven gas supply shut-off valve (2)

Figure 3: Shut-off valve integrated at the end-wall of the driver section of the shock tube used for venting the driver gas to the atmosphere

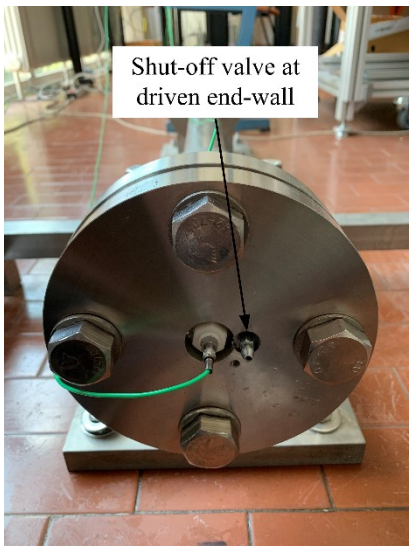

Figure 4: Shut-off valve integrated at the end-wall of the driven section of the shock tube used for venting the driven gas to the atmosphere

3. RESULTS

The study of the generated pressure steps in the shock tube using different combinations of lower- and higher-molecular-weight gases as driver and driven gas was carried out with chemically inert gases; helium (He) as a lower-molecular-weight gas, and nitrogen (N_2) and argon (Ar) as a higher-molecular-weight gas. The pressure steps generated with each combination of the gases were carried out at the atmospheric initial driven pressure p_1 and at the initial driver gauge pressure $p_{4,g}$ from 4 MPa to 10 MPa (both measured with a pressure transducer Mensor, CPR6000), where each measurement was repeated three times. The properties of the used driven gases, which determine the amplitude of the generated pressure steps at the end-wall of the driven section (see equation (1)), for different

studied combinations of the driver-driven gases were obtained from the NIST REFPROP database [6] for p_1 and T_1 conditions and are presented in Table 1 to Table 4.

Table 1: Properties of driven He (gas combination He-He)

$p_{4,g}$ MPa	Rep.	p_1 MPa	γ_1	a_1 m/s
4	1	0.09768	1.667	1018
4	2	0.09768	1.667	1018
4	3	0.09768	1.667	1019
6	1	0.09778	1.667	1018
6	2	0.09778	1.667	1018
6	3	0.09778	1.667	1018
8	1	0.09778	1.667	1019
8	2	0.09778	1.667	1018
8	3	0.09778	1.667	1018
10	1	0.09798	1.667	1017
10	2	0.09798	1.667	1017
10	3	0.09798	1.667	1016

Table 2: Properties of driven N_2 (gas combination N_2-N_2)

$p_{4,g}$ MPa	Rep.	p_1 MPa	γ_1	a_1 m/s
4	1	0.09844	1.401	353.1
4	2	0.09843	1.401	353.1
4	3	0.09842	1.401	353.1
6	1	0.09836	1.401	353.1
6	2	0.09835	1.401	353.1
6	3	0.09835	1.401	353.1
8	1	0.09830	1.401	353.0
8	2	0.09826	1.401	352.9
8	3	0.09827	1.401	352.8
10	1	0.09823	1.401	353.2
10	2	0.09822	1.401	353.2
10	3	0.09819	1.401	353.2

Table 3: Properties of driven N_2 (gas combination He-N_2)

$p_{4,g}$ MPa	Rep.	p_1 MPa	γ_1	a_1 m/s
4	1	0.09786	1.401	353.1
4	2	0.09782	1.401	353.0
4	3	0.09782	1.401	353.0
6	1	0.09782	1.401	353.0
6	2	0.09782	1.401	353.0
6	3	0.09778	1.401	352.9
8	1	0.09850	1.401	354.0
8	2	0.09850	1.401	353.9
8	3	0.09850	1.401	353.9
10	1	0.09787	1.401	353.5
10	2	0.09787	1.401	353.5
10	3	0.09787	1.401	353.5

Table 4: Properties of driven Ar (gas combination He-Ar)

$p_{4,g}$ MPa	Rep.	p_1 MPa	γ_1	a_1 m/s
4	1	0.09766	1.669	323.7
4	2	0.09766	1.669	323.6
4	3	0.09773	1.669	323.6
6	1	0.09778	1.669	323.8
6	2	0.09780	1.669	324.0
6	3	0.09790	1.669	323.5
8	1	0.09757	1.669	323.9
8	2	0.09757	1.669	323.7
8	3	0.09757	1.669	323.6
10	1	0.09787	1.669	323.5
10	2	0.09784	1.669	323.9
10	3	0.09804	1.669	323.2

Figure 5 shows the end-wall shock wave velocities V generated with different gas combinations. From the figure it is seen that the highest V are generated with He-He, where V increases from approximately 1641 m/s to 1921 m/s when increasing $p_{4,g}$ from 4 MPa to 10 MPa. In combinations of He-N_2 or He-Ar, the results of generated shock wave velocities are nearly similar and increase from approximately 800 m/s to 1018 m/s in average for both gas combinations. The lowest V on the other hand is generated with the combination N_2-N_2. The end-wall shock wave velocities in this case increase from approximately 626.9 m/s to 713.6 m/s.

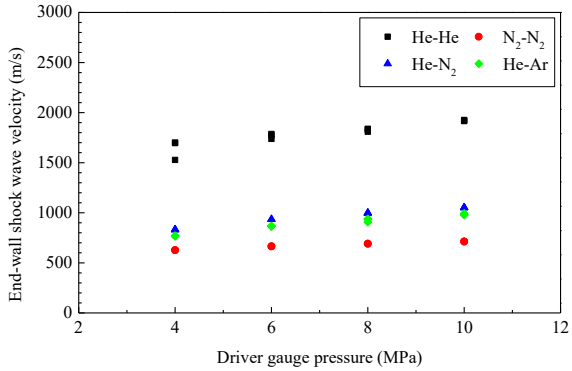

Figure 5: Generated end-wall shock wave velocities at different initial driver gauge pressures for different combinations of gases

Figure 6 shows the generated end-wall shock wave Mach numbers M. Although the generated V are the highest for He-He (see Figure 5), due to approximately three times higher speed of sound in the driven He with respect to the speed of sound in the driven N_2 or Ar (see Table 1 to Table 4) that results from smaller molecular weight of He, M for these combination of gases become the lowest with respect to other combinations of gases and increases from approximately 1.6 to 1.9. While for the combination N_2-N_2 the generated M are slightly

higher than for the combination He-He, much higher M are achieved with the combination of He-N_2 or He-Ar. While M achieved with the combination of He-N_2 are in average approximately 1.4 times larger for all the initial pressures than M generated with the combination of N_2-N_2 (the ratio of the obtained M is approximately the same as the ratio of the obtained V due to approximately the same speed of sound in the driven N_2 for both combinations of gases), M achieved with the combination of He-Ar are in average by 1.4 % larger than M achieved with He-N_2 and increase from approximately 2.4 to 3 when increasing $p_{4,g}$ from 4 MPa to 10 MPa.

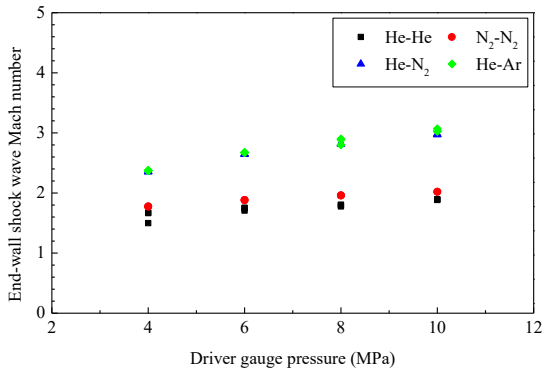

Figure 6: Generated end-wall shock wave Mach numbers at different initial driver gauge pressures for different combinations of gases

Figure 7 shows the amplitudes of the pressure steps generated at the end-wall Δp which are obtained with equation (1). The trends of the generated Δp are similar as they are for M, where the lowest Δp are achieved with the combination of He-He and slightly higher Δp with the combination of N_2-N_2. Much higher Δp are achieved with the combinations of He-Ar and He-N_2. With the combination of He-Ar obtained Δp are in average approximately three times larger than Δp generated with N_2-N_2. Although the generated M are slightly higher for the combination of He-Ar with respect to the combination of He-N_2 (see Figure 6), Δp generated with He-N_2 are higher for 2.6% in average for all the initial pressures due to lower adiabatic index γ_1 of driven N_2 with respect to γ_1 of the driven Ar at approximately the same initial conditions (see Table 3 and Table 4).

Figure 8 shows the reference pressure step signals determined at the end-wall of the driven section with the equations (1) and (2) for all the studied combinations of the gases at $p_{4,g}$ = 10 MPa and the corresponding DUT's output voltage signals.

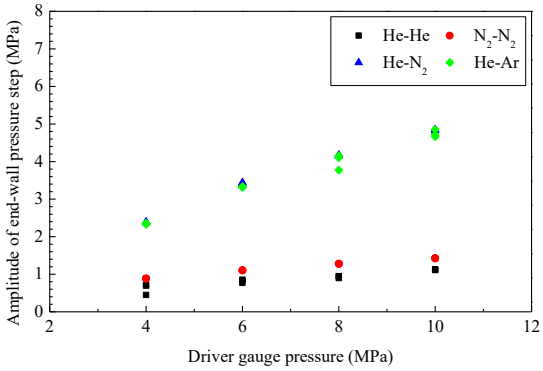

Figure 7: Amplitudes of the generated end-wall pressure steps at different initial driver gauge pressures for different combinations of gases

The signals are shown for the interval from –0.1 ms to 0.5 ms, where the arrival time of the shock front at the end-wall t_{wall} is set to $t = 0$. From the figure it is seen that the Δp generated in the shock tube with He-He is in average approximately 1.1 MPa, with N_2-N_2 1.4 MPa, with He-Ar 4.7 MPa and with He-N_2 4.8 MPa. The resulting DUT's response signals reach their final post-shock average value within 0.5 ms after the generated pressure step change for all the observed combinations of gases, where the final response value increases almost proportionately with the amplitude of the reference pressure signal from approximately 1.2 V for He-He to 4.8 V for He-N_2.

4. CONCLUSIONS

According to industrial and scientific requirements the aim of this paper was to increase the amplitude range of the pressure steps generated in the straight diaphragmless shock tube with constant inner diameter by using different gases in the driver and driven section. The results show that for each driver-driven gas combination the generated V increase almost linearly with increasing initial driver gauge pressure $p_{4,g}$ while holding p_1 at nearly constant pressure. For the given $p_{4,g}$ the generated V increase with the increasing a_1, a_4/a_1, where a_4 is the speed of sound in the driver gas, and γ_1. The highest V are therefore generated with the combinations of He-He due to much higher a_1 of He used as driven gas with the respect to N_2 and Ar used as driven gases in other combinations. The generated V with the combinations of He-N_2 or He-Ar are similar, while the lowest V are generated with the combination of N_2-N_2 due to relatively low a_4/a_1 and γ_1 with respect to other combinations of gases.

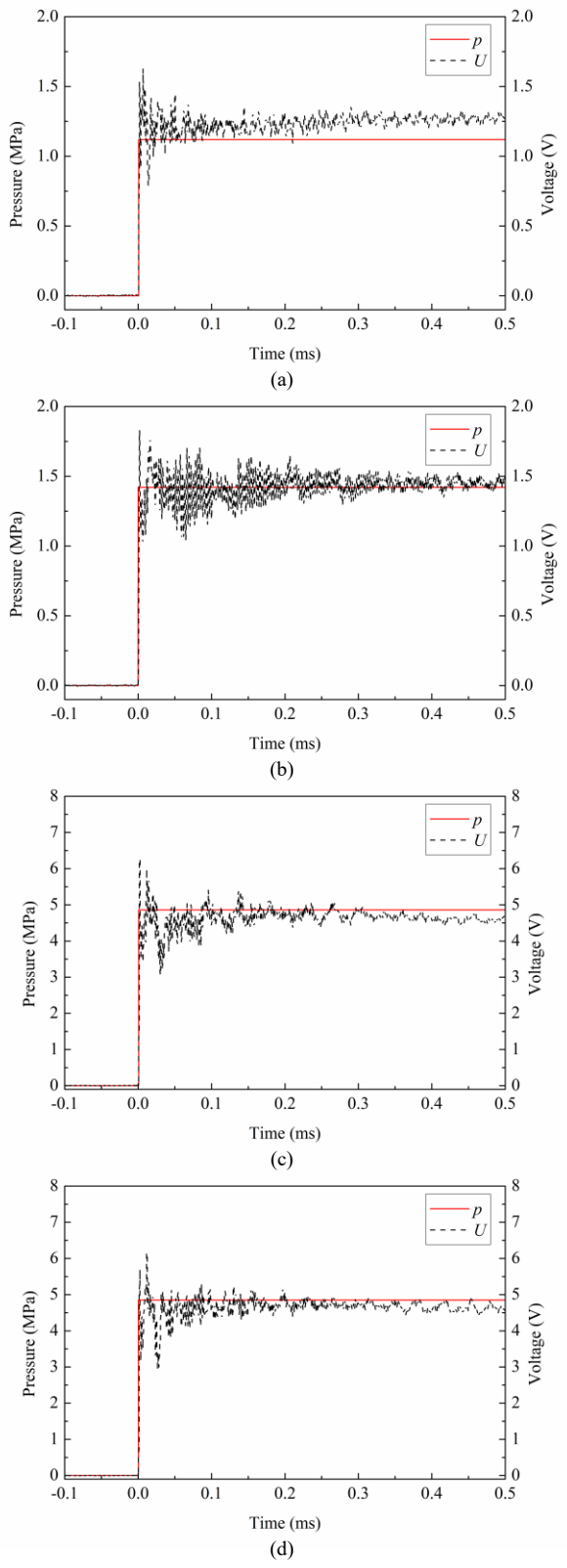

Figure 8: Generated end-wall gauge pressure and the corresponding DUT's output voltage signal at $p_{4,g}$ = 10 MPa; (a) He-He, (b) N_2-N_2, (c) He-N_2, (d) He-Ar

The results of the obtained M on the other hand show that for the given $p_{4,g}$ the generated M increase with a_4/a_1. The highest M are therefore achieved when using lower-molecular-weight driver gases and higher-molecular-weight driven gases, i.e., He-N_2 or He-Ar. The trends of the generated Δp are similar to the generated M, only that Δp generated with He-N_2 become slightly larger than with He-Ar due to lower adiabatic index γ_1 of driven N_2 with respect the driven Ar. This study concludes that the combinations of lower-molecular-weight driver gas and higher-molecular-weight driven gas, i.e., helium for the driver gas, and argon or nitrogen for the driven gas, increase the generated pressure steps by at least 3 times in comparison to other combinations of gases, i.e., He-He or N_2-N_2.

ACKNOWLEDGEMENTS

The authors acknowledge the financial support of the Slovenian Research Agency for the project Advanced shock tube system for high-frequency primary dynamic pressure calibration (project No. J2-3054), in addition to the research core funding (No. P2-0223).

REFERENCES

[1] J. Hjelmgren, Dynamic Measurement of Pressure - A Literature Survey. Borås: SP Swedish National Testing and Research Institute, 2002.

[2] A. Svete, J. Kutin, "Characterization of a Newly Developed Diaphragmless Shock Tube for the Primary Dynamic Calibration of Pressure Meters", Metrologia, vol. 57, no. 5, 2020, 055009. DOI: 10.1088/1681-7575/ab8f79

[3] A. Svete, J. Kutin, "Identifying the High-Frequency Response of a Piezoelectric Pressure Measurement System Using a Shock Tube Primary Method", Mech. Syst. Signal Process, vol. 162, 2022, 108014. DOI: 10.1016/j.ymssp.2021.108014

[4] A. Svete, F. J. Hernández Castro, J. Kutin, "Effect of the Dynamic Response of a Side-Wall Pressure Measurement System on Determining the Pressure Step Signal in a Shock Tube Using a Time-of-Flight Method", Sensors, vol. 22, 2022, no. 6, 2103. DOI: 10.3390/s22062103

[5] D. W. Holder, D. L. Schultz, On the Flow in a Reflected-Shock Tunnel. London: Her Majesty's Stationery Office, 1962.

[6] E. W. Lemmon, M. L. Huber, M. O. McLinden, NIST Standard Reference Database 23: Reference Fluid Thermodynamic and Transport Properties – REFPROP, ver. 9.0. Gaithersburg: National Institute of Standards and Technology, 2010

.